TELKOMNIKA, Vol. 16, No. 5, October 2018, pp. 2275~2286
ISSN: 1693-6930, accredited First Grade by Kemenristekdikti, Decree No: 21/E/KPT/2018
DOI:10.12928/TELKOMNIKA.v16i5.7028

Combination of Flex Sensor and Electromyography for Hybrid Control Robot

Muhammad Ilhamdi Rusydi*[1], Muhammad Ismail Opera[2], Andrivo Rusydi[3], Minoru Sasaki[4]
[1,2]Department of Electrical Engineering, Universitas Andalas, Padang, Indonesia
[3]Department of Physics, National University of Singapore, Singapore
[4]Department of Mechanical Engineering, Gifu University, Japan
e-mail: rusydi@eng.unand.ac.id

Abstract

The alternative control methods of robot are very important to solved problems for people with special needs. In this research, a robot arm from the elbow to hand is designed based on human right arm. This robot robot is controlled by human left arm. The positions of flex sensors are studied to recognize the flexion-extension elbow, supination-pronation forearm, flexion-extension wrist and radial-ulnar wrist.The hand of robot has two function grasping and realeasing object. This robot has four joints and six flex sensors are attached to human left arm. Electromyography signals from face muscle contraction are used to classify grasping and releasing hand. The results show that the flex sensor accuracy is 3.54˚ with standard error is approximately 0.040 V. Seven operators completely tasks to take and release objects at three different locations: perpendicular to the robot, left-front and right-front of the robot. The average times to finish each task are 15.7 ssecond, 17.6 second and 17.1 second. This robot control system works in a real time function. This control method can substitute the right hand function to do taking and releasing object tasks.

Keywords: *robot, flex sensor, electromyography, left arm*

1. Introduction

The aging society gives impact to the demand of exoskeleton robots such as human arm. So, this mechanics is frequently discussed in robotics because of its important functions [1,2,3,4]. A simple 1-DoF exoskeleton robot was designed and controlled by electromyography (EMG) [5]. A robot manipulator was controlled by electrooculography (EOG) to reach an object [6].

In many aspects, robot and human can work together in manufacturing as long as the communications between them are established. Robot can also reduce the risk on the workers such as fire fighters [7] Althought the communication methods linking them are limited, gesture recognition gives wide applications to for human robot interaction [8,9,10]. Human gesture makes the communication between robot and human could be further developed. A robot for writing and painting tasks was developed and controlled by human gesture. A database of human gestures for English and Chinesse characters was created using Microsoft Kinect. A robot used this database to recognize the human gesture in real time then performed the gesture to write the characters [11]. A remote control of mobile robot was also developed by [12] using virtual reality and audio based control [13].

Biosignals such as electromyography (EMG) and electroencephalography (EEG) become very famous in this decade because of this ability to control machine instead using the hands [14]. An antropomorphic prosthetic hand was controlled by voice in medical system [15]. But some people with problem with their articulation still can use EMG signal control robot by as the alternative method [16]. If a human body has a total health problem, EEG signal become the last signal that still can be produced by human body. Four mental tasks were clustered by Support Vector Machine to control robot arm [17]. The combination of EMG signal and encoder sensor to control robot arm is established with accuracy is approximately 9° [18].

Since robot technology grows rapidly to help people in daily life acitivities, the method to control the robot by human is very important because of different abilities among the users who operate the robot. Some aspects are discussed about the interaction of robot and human such as accuracy and speed to execute task [19]. A Human Robot Interaction (HRI) based on gesture control was introduced [20]. This robot is able to recognize four gestures: wave hand, pointing at,

Received August 20, 2017; Revised April 17, 2018; Accepted May 21, 2018

head shake and nod. The gesture was capture by Microsoft Kinect. The response speed and the recognition rate were evaluated. In average, the execution time was between 1.5 second and 2 second. The point gesture had the highest recognition rate (96.67%) and the negate gesture had the lowest rate (33.33%). This robot sometimes went to the wrong places (13.33%).

Instead of using optic sensors to capture the human gesture, flex sensor give an alternative method for this function. The resistance value of it depends on the angle of bending. The arrangement of flex sensors to a goniometric glove is very usefull to build the pattern of finger gestures. The repeatability and degree of handling of the flex sensors arrangement are tested by 6 subjects [21]. The results showed that the average range of flex sensors output was 3.27° with 1.07° standard deviation. This output range is very important for the system accuracy.

In this study, a human arm is controlled by the combination of flex sensor and EMG. The flex sensor arrangements to the human arm are estabilished. The accuracy was of flex sensor was evaluated. The EMG distinguishes the grasping and relaxing hand based on threshold value. The robot control system was tested by seven subjects for three tasks.

2. Method

2.1. Arm Motions

The right arm robot is developed in order to help people with the right arm problem to reach objects on the right side of their body. So, the basic movements of right arm are required to develop this robot. In this study, hand damage is assumed to occur from elbow to fingers. The Figure 1(a) to (d) illustrates the movements of joint in that section. An elbow allows the arm to rotate by θ_1 from the extension to the flexion position on a plane as shown by Figure 1(a).The angle increases when the flexion occurs and the angle decreases if the movement is an extension. The other important movement near the elbow is the rotation by θ_2 from the supination to the pronation as shown by Figure 1(b). Extension and flexion are not only at the elbow but also at the wrist as shown by Figure 1(c). The angle for the extension to the normal position is θ_3 and the angle for the flexion to the normal position is θ_4. The last couple movements at the wrist are the radial and ulnar as illustrated by Figure 1(d). The radial movement is the hand movement about θ_5 degree towards the kinky finger and its opposite is the ulnar movement with angle θ_5 to the normal position. All these features drive the hand moving from an initial position to a target position. For the grasping function, the hand has two conditions: release and hold as shown by Figure 2.

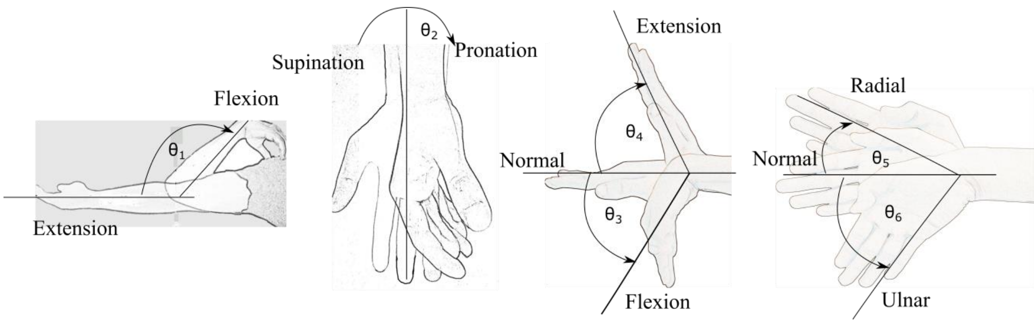

(a) (b) (c) (d)

Figure 1. The hand movement from elbow to the wrist section

Figure 2. Two conditions of arm: relase and hold

2.2. Right Arm Robot

Considering the assumed problem of the hand in this research, the arm robot only consists of the elbow, wrist and hand. To fulfill the requirement of the arm movement, a robot is designed as illustrated by Figure 3. The first joint on the elbow is operated by motor 1. The configuration of this motor producesthe θ_1 for the elbow flexion and extension. The motor for the second joint rotates the hand for pronation and supination. For the wrist function, two motors are installed for the radial and ulnar (motor 3) and flexion and extension (motor 4). The specification of four joints and four links links are shown by Table 1 and Table 2 respectively.

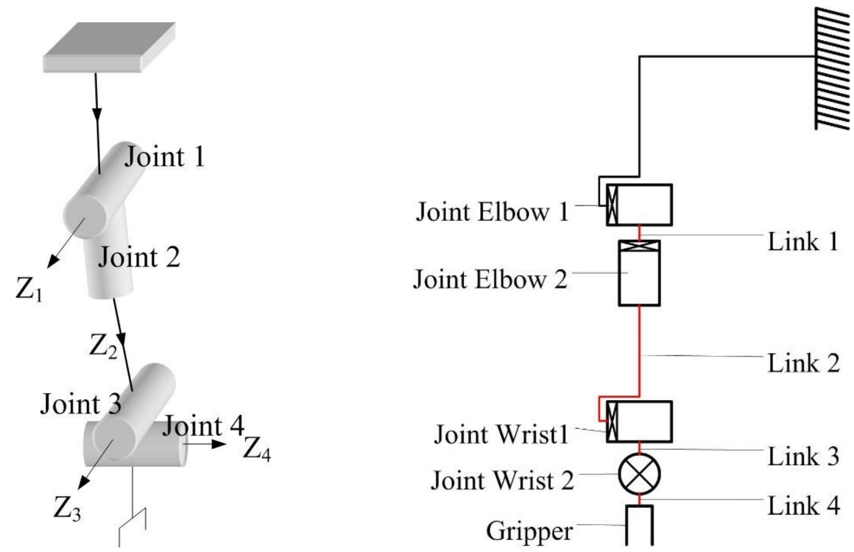

Figure 3. Four joints of the robot

Table 1. The Joint Specification

Segment	Joint	Code	Movement	Workspace	Actuator
Elbow	1	A	Flexion	0°-150°	Servo FeeTech
		B	Extension		FR0115M
	2	C	Supination	0°-180°	(Torque: 14 kgcm)
		D	Pronation		
Wrist	3	E	Flexion	60°	
		F	Extension	80°	
	4	G	Radial	30°	
		H	Ulnar	60°	

Table 2. Length of Link

Link	Length (cm)
Link 1	2
Link 2	9
Link 3	5
Link 4	6

2.3. Hand Gesture Sensor

Flex sensors are used to detect the hand gesture in this research. This type of sensors is produced by Spectrasymbol. It is a high resistance flex sensor that possibly works in a temperature ranges from -35°C to 80°C. This produced sensor has two length types which are 4.4 cm and 2.5 cm. The flat resistance of 4.4 cm flex sensor is about 10 KΩ and the flat resistance for 2.5 cm flex sensor is about 22 KΩ. In general, the flat resistance for bending angle 180° is about two times greater than the flat resistance. The basic electrical circuit of the flex sensor is shown in Figure 4. Since it works as the voltage divider, the value of the R_1 is designed equal to the flat resistance of each sensor types. The output of the flex sensor is denoted as FS. Further, this variable is used to determine the bending angle of flex sensor.

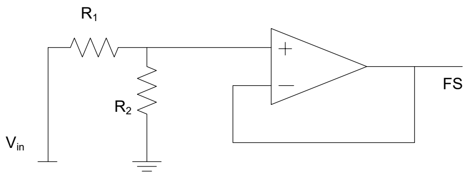

Figure 4. Electrical circuit of flex sensor.

Because the idea of this robot is to help people with right hand problem, this robot is available controlled by human left hand only. The installation of the flex sensors is investigated to make the sensor that can determine the angles of the four joints. Two joints on the elbow and two joints on the wrist of the robot are directly modeled based on the elbow and wrist part of human left hand. The flex sensors are attached gently on the locations as in Figure 5. Location number 1 is the location for flex sensor 1. This flex sensor is influenced by the elbow flexion and extension. Flex sensor 2 detects the pronation and supination. Flex sensor 3 and 4 distinguish the flexion and estension at the wrist. Flex sensor 5 and 6 identifies the radial and ulnar. The relationship between each sensors and the joint movement are summarized in Table 3.

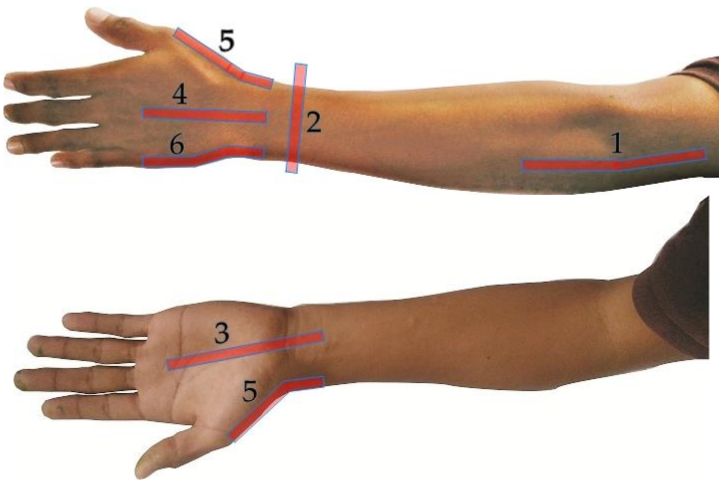

Figure 5. The positions of flex sensors

Table 3. The Mapping of Flex Sensor to the Joint Movement

Joint	Code	Movement	Flex sensor
1	A	Flexion	1
	B	Extension	
2	C	Supination	2
	D	Pronation	
3	E	Flexion	3
	F	Extension	4
4	G	Radial	5
	H	Ulnar	6

A different design is implemented to the sensor 2. This is because the pronation and supination rotation are different with other rotations. For the flex sensor 2, a tool with a hole that can fit with human left arm is designed. A flex sensor is attached on the bottom of the hole with one side is fixed and other side is the moving part. The flex is flat when the hand on the supination movement and it curves when the hand is on pronation movement, as shown in Figure 6.

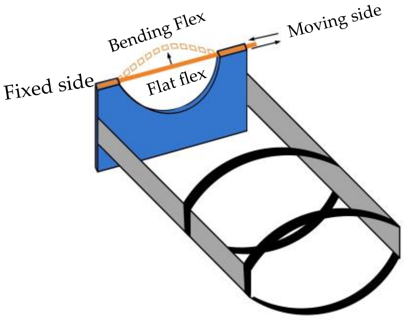

Figure 6. Design of flex sensor 2

2.4. Electromyography

The electromyography sensor used in this research is an open source and hardware product version 1.3 leaded by Backyardbrain. It has 80× gain amplifier for the band pass filter 300 Hz – 1200 Hz. The sampling rate is 10 Hz. There are three cables as input which are red (positive), black (negative) and white (ground) channel. The signal from the muscle around the face is used to control the robot. The electrodes are attached at the jaw as shown in Figure 7.

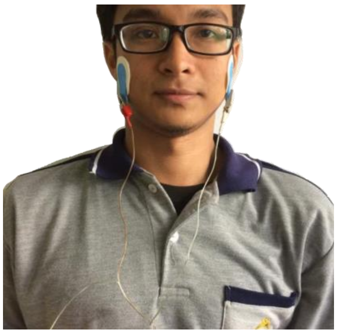

Figure 7. Electrode positions of EMG sensor

The EMG signal is used for a simple task since the hand of robot operated only in grasping and releasing without considering the power of grasping. So, the threshold method is used to classify the situation. The threshold is studied based on three experiments. First, the experiment is to investigate the peak of the EMG. The subjects performed the jaw contraction just only for a moment. This experiment is important to determine the threshold value. After that, caused of the used of EMG signal, the experiment to study the stability of EMG signal is studied. Subjects performed the jaw contraction and hold the contraction with two durations: 5 seconds and 15 seconds. This experiment is necessary to investigate that EMG signal can stand above the threshold value for those durations.

2.5 Control Method

The developed system works in a real time operation. The robot follows the human left arm movement and the robot hand grabs or releases object based on the face muscle contraction. There are two main parts of the system to control the robot manipulator using this hybrid sensor designed, as presented in Figure 8. The first part is to detect the arm movement and calculate the joint angle. This part consists of 6 flex sensors and an EMG sensor connects to a microcontroller. In the first microcontroller, the voltage outputs of the flex sensors are manipulated into the angles. These angles together with the EMG signals are transmitted to other system through nRF24L01. On the microcontroller 2, the angle of six flex sensors are processed to decided the angles of four robot joints. Based on the EMG signal, the microcontroller 2 decides whether the hand grasps or releases the object.

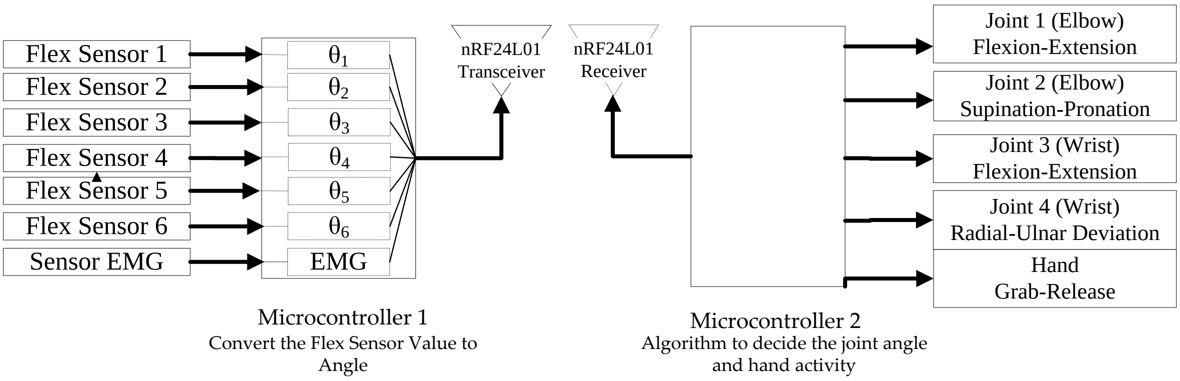

Figure 8. Architecture of control system to control four joints and flexor muscle

Figure 9 illustrates the process on the microprocessor 1. The minimum and maximum output (FS_{i_min} and FS_{i_max}) of flex sensors are declared at the initialization step. The minimum value is the output of the flex sensor when the arm posed in straight down position which is the initial position. The system reads the bending values of six flex sensors (FS_i) and EMG signal amplitude. Then, the bending values are converted to the bending angles of six flex sensors. The relationship between the bending value (FS_i) and the bending angle (θ_i) are determined based on the (1). The bending angles of the flex sensors and the EMG amplitude are sent to the microprocessor 2.

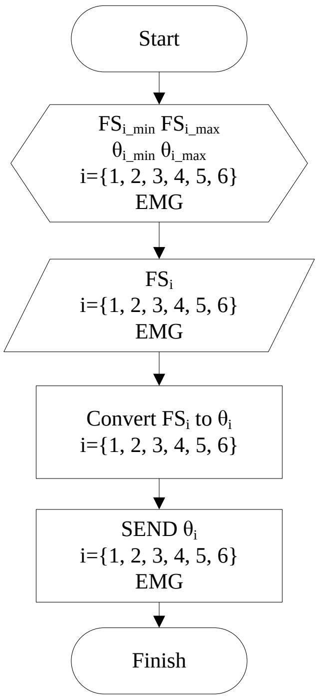

Figure 9. The process for input and output on microprosesor 1

$$\theta_i = \overline{\theta_{i\_min}} + \left(FS_i - \overline{FS_{i\_min}}\right)\left(\frac{\overline{\theta_{i\_max}} - \overline{\theta_{i\_min}}}{\overline{FS_{i\_max}} - \overline{FS_{i\_min}}}\right) \quad (1)$$

where

i : Flex sensor number (1, 2, 3, 4, 5, 6)
θ_i : Bending angle of flex sensor i (°)
$\overline{\theta_{i\_min}}$: The minimum bending angle of flex sensor i (°)
$\overline{\theta_{i\_max}}$: The maximum bending angle of flex sensor i (°)
FS_i : The flex sensor i signal (mV)
$\overline{FS_{i\_min}}$: The minimum flex sensor i signal (mV)
$\overline{FS_{i\_max}}$: The maximum flex sensor i signal (mV)

The output of the microprocessor 1 is the input for the microprocessor 2. The process in microprocessor 2 is shown by Figure 10. The declaration of the EMG threshold value is initiated in this section. If the the EMG signal is bigger than the EMG threshold (EMG_{th}), the hand grasps the object. The hand releases the object if the EMG signal is lower than the threshold.

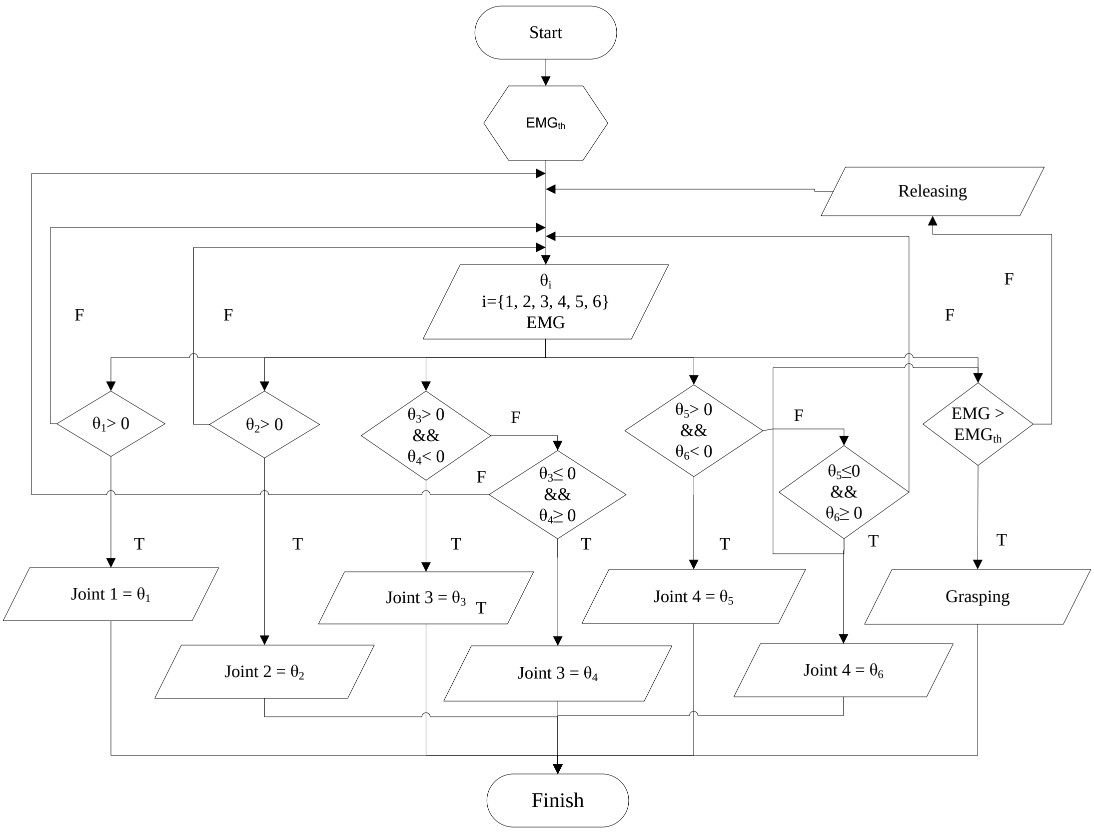

Figure 10. The process for input and output on Microprossor 2

3. Result And Discussion

3.1. EMG Threshold

The experiment to determine the threshold was conducted by 9 subjects. The subjects contracted their jaws for a moment for five times. The maximum value of the EMG signal was recorded. The averages of maximum values of the EMG signal while the subjects were biting their jaw for a moment are shown by Figure 11. In a glance, this experiment showed that the biting activity had an average maximum EMG value which was bigger than 200 μV. Based on this experiment, 100 μV was decided to differentiate the grasping and releasing hand.

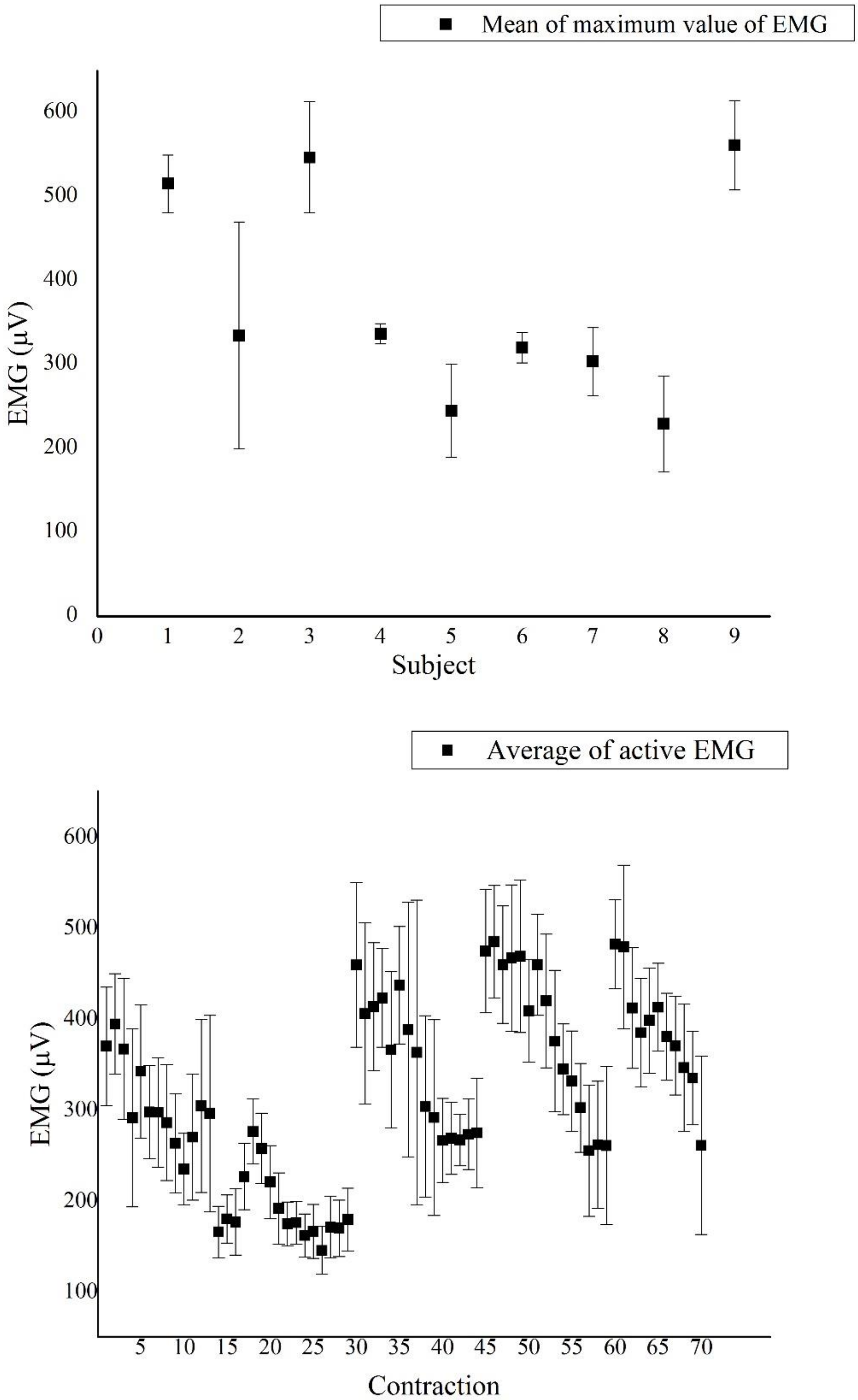

Figure 11. Mean of maximum value of EMG for instantaneously jaw contraction

The decided threshold value was evaluated by holding the contraction for 15 seconds. Totally 70 contractions were performed by random 10 subjects. The result illustrates by Figure 11. The average EMG value during the five second contraction varied between about 150 μV and 500 μV. This figure shows that EMG value can be maintained above the threshold for five second contraction. It means that the subject can handle the object for some moments. But, Figure 12 also shows that the amplitude of EMG value had decending pattern during the 15 seconds holding contraction. For that period, the EMG is still bigger that the threshold value but it could decrease around 75% from the initial value. In order to keep this value bigger than the threshold, the maximum holding contraction respectively is only about 15 seconds.

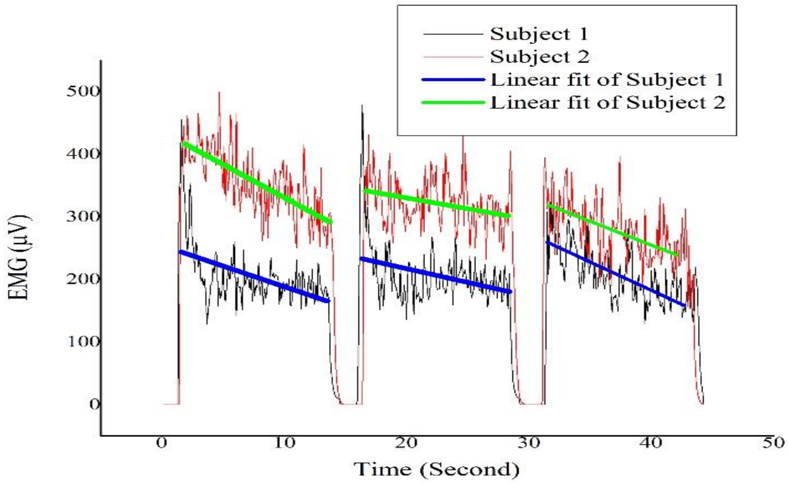

Figure 12. The trend of EMG signal for 15 seconds contraction

3.2. Flex Sensor

The characteristic of the flex sensors affected by the bending angle and the center of curvature was investigated. Three centers of curvature for 2.2 inch flex sensor and four centers of curvature were studied to understand their influence to the flex sensor output. The curvature centers for 2.2 inch flex sensor were 25%, 50% and 75%. As the 4.5 inch flex sensor are longer, so the investigated curvature centers were 20%, 40%, 60%, and 80% as illustrated by Figure 13. The 25% of curvature center for 2.2 inch flex sensor meant that the flex sensor was bended on 0.55 inch from the base of flex sensor. In the same way, the 20% curvature center for 4.5 cm meant that the bending happened on 0.9 inch from the base. The flex sensors voltage output for 0˚, 10˚, 20˚, 30˚, 40˚, 50˚, 60˚, 70˚, 80˚, 90˚ and 180˚bending angle were determined with 5 volt voltage input. The resistances (R_1) for the voltage devider were equal to the flat resistance of each sensor types.

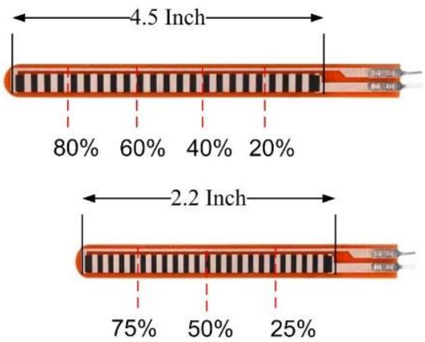

Figure 13. The investigated center of curvature of flex sensors

The result shows that the slope voltage to the bending angles for all centers of curvature is about 0.01 for both types, as in Figure 14(a) and Figure 14(b). In average, the standard error of the 2.2 inch flex sensor in the intercept line is about 0.037 V. This figure is relatively close to the standard error for 4.4 inch flex sensor which is 0.030 V. With the average range of voltage output between 10˚ and 90˚ bending angle is about 0.9 V, so the accuracy is approximately 3.54˚ with assumption that the average of standard error is 0.040 V for both flex sensor types. Based on that result, if the $\overline{\theta_{i\_min}}$ is equal to 0˚, so the $\overline{FS_{i\_min}}$ is always 2.5 volt. The values of $\overline{FS_{i\_max}}$ is determined based on the maximum angle of hand movement of each joints ($\overline{\theta_{i\_max}}$).

The characteristics of these sensors are same for all curvature centers. Subjects can bend the flex sensors in moveable location. But in this research, the used points are only between 40% and 60% bending center. Although in general the voltage output is linear to the bending angle, but the 2.2 Inch flex sensor has rapidly increases of voltage output from the 0˚ and 90˚ bending angle. Compare to the 4.4 Inch flex sensor this situation could be related to the flexibility of the sensor. The shorther of the sensor, the harder to bend it.

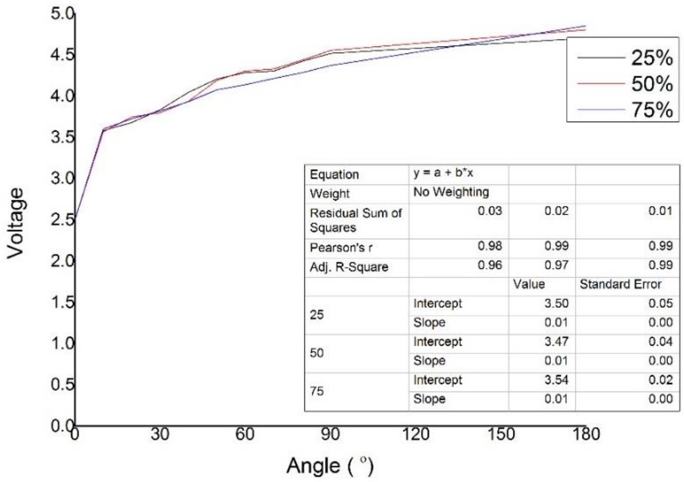

Equation	y = a + b*x		
Weight	No Weighting		
Residual Sum of Squares	0.03	0.02	0.01
Pearson's r	0.98	0.99	0.99
Adj. R-Square	0.96	0.97	0.99
		Value	Standard Error
25	Intercept	3.50	0.05
	Slope	0.01	0.00
50	Intercept	3.47	0.04
	Slope	0.01	0.00
75	Intercept	3.54	0.02
	Slope	0.01	0.00

(a)

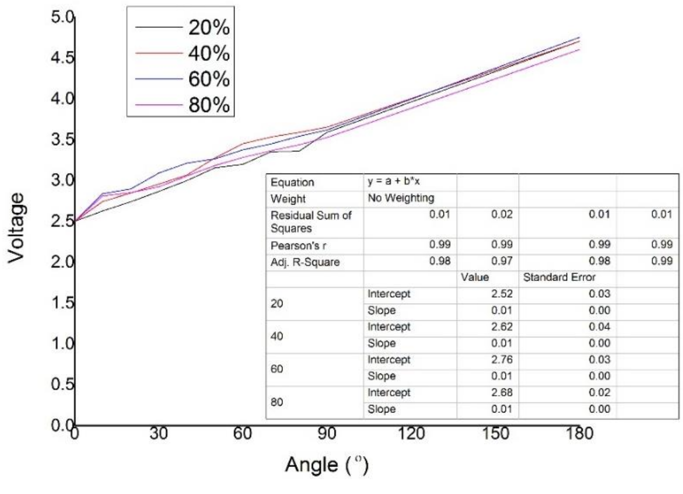

Equation	y = a + b*x			
Weight	No Weighting			
Residual Sum of Squares	0.01	0.02	0.01	0.01
Pearson's r	0.99	0.99	0.99	0.99
Adj. R-Square	0.98	0.97	0.98	0.99
		Value	Standard Error	
20	Intercept	2.52	0.03	
	Slope	0.01	0.00	
40	Intercept	2.62	0.04	
	Slope	0.01	0.00	
60	Intercept	2.76	0.03	
	Slope	0.01	0.00	
80	Intercept	2.68	0.02	
	Slope	0.01	0.00	

(b)

Figure 14. The relationship between the bending angle, center of curvature and the voltage of (a) 2.2 inch and (b) 4.5 inch flex sensor

3.3 System Evaluation

The integrated system as shown by Figure 15(a) was evaluated based on the time consumed by the seven subjects to perform the tasks. Three objects were hanged in front of the robot as shown by Figure 15(b) with three locations, perpendicular to the robot based as shown by Figure 15(c), right front as shown by Figure 15(d) and left front as shown by Figure 15(e). The subject operated the robot from the initial position to grab the object and move the robot to the initial position before releasing the object from the hand. The time consume to finish the task is presented by Table 4. The result shows that all subjects can do the task for all trials. The average times to finish the 1st, 2nd and 3rd tasks are about 15.7 second, 17.1 second 17.6 second. It shows that the simplest task is when the object is perpendicular to the robot base. The subject only operates the robot with the flexion elbow and wrist. The 2nd and 3rd experiments are more difficult, because these locations need radial and ulnar movement. In this situation, it is rather difficult to estimate the object position to the robot hand. The subject usually misses the object because of the unaccurate estimation of the distance.

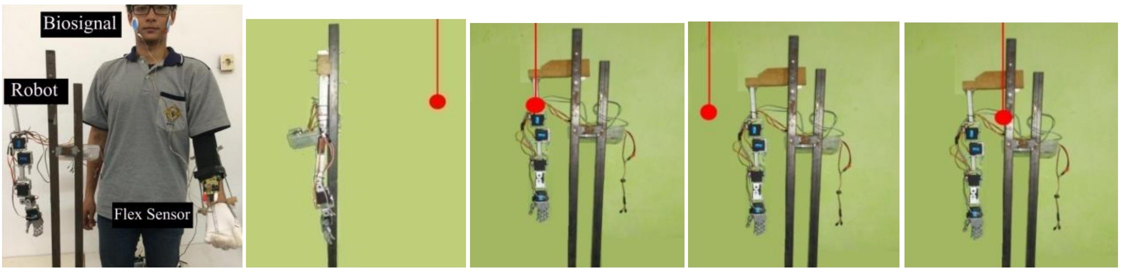

(a) (b) (c) (d) (e)

Figure 15. (a) integrated system, (b) the object from the robot side, (c) object perpendicular to the robot base, (d) right front object and (e) left front object.

Table 4. System testing with three object locations.

Subject	Time (Second)		
	Perpendicular Experiment	Right Front Experiment	Left Front Experiment
1	14	16	17
2	15	17	20
3	15	18	17
4	16	17	17
5	17	19	19
6	17	15	14
7	16	18	19

4. Conclusion

In this research, the arrangement of flex sensors to determine the right hand movement from elbow to wrist is established. Six flex sensors are used for elbow flexion and extension, pronation, supination, hand flexion, hand extension, hand radial and hand ulnar. The EMG signals are used to differentiate grapsping and relasing hand. This robot can follow the human arm motions in a real time control. Seven subjects successfully operated this robot to grasp and release objects in three different locations.

Acknowledgment

This research funded by Hibah Publikasi, Engineering Faculty, Universitas Andalas under Conctrat No. 023/UN.16.05.D/PL/2018.

References

[1] Meiling Wang, Minzhou Luo, and Marco Ceccarelli. A Unified Dyanamic Conctrol Method for a Redundant Dual Arm Robot. *Journal of Bionic Engineering*. 2015; 12: 361-371.
[2] Aihui Wang, Hongnian Yu, Cang, and Shuang. Bio-inspired robust control of a robot arm-and-hand system based on human viscoelastic properties. *Journal of the Franklin Institute*. 2017; 354: 1759-1783.
[3] Chang-Hyuk Lee, Jiwon Choi, Hooman Lee, Joongbae Kim, Kyung-min Lee and Young-bong Bang. Exoskeletal master device for dual arm robot teaching. *Mechatronics*. 2017; 43: 76-85.
[4] Erol Ozgur and Youcef Mezouar. Kinematic modeling and control of a robot arm using unit dual quaternions. *Robotics and Autonomous Systems*. 2016; 77: 66-73.
[5] Masashi Hamaya, Takamitsu Matsubara, Tomoyuki Noda, Tatsuya Teramae, and Jun Morimoto. Learning assistive strategies for exoskeleton robots from user-robot physical interaction. *Pattern Recognition Letters*. 2017; 99: 1-10.
[6] Muhammad Ilhamdi Rusydi, Takeo Okamoto, Satoshi Ito, and Minoru Sasaki. Controlling 3-D Movement of Robot Manipulator using Electrooculography. *International Journal on Electrical Engineering and Informatics*. 2017; 10: 170-185.
[7] Ihsan A. Taha and Hamzah M. Marhoon. Implementation of Controlled Robot for Fire Detection and Extinguish to Closed Areas Based on Arduino. *Telkomnika*. 2018; 16(2): 654-664.
[8] Hongyil Liu and Lihui Wang. Gesture recognition for human-robot collaboration: A review. *International Journal of Industrial Ergonomics*. 2017; Article in Press: 1-13.
[9] Mei Wang, Wen-Yuan Chen, and Xiang Dan Li. Hand gesture recognition using valley circle feature and Hu’s moments technique for robot movement control. *Measurement*. 2016; 94: 734-744.
[10] Ram Pratap Sharma and Gyanendra K Verma. Human Computer Interaction using Hand Gesture. *Procedia Computer Science*. 2015; 54: 721-727.
[11] Fei Chao, Yuxuan Huang, Xin Zhang, Changjing Shang, Longzhi Yang, Changle Zhou, Huosheng Hu and Chih-Min Lin. A robot calligraphy system: From simple to complex writing by human gestures. *Engineering Applications of Artificial Intelligence*. 2017; 59: 1-14.
[12] Ibari Benaoumeur, Ahmed-Foitih Zoubir, and Hanifi Elhachimi Amar Reda. Remote Control of Mobile Robot using the Virtual Reality. *International Journal of Electrical and Computer Engineering*. 2015; 5(5): 1062-1074.
[13] Xuan Bokai, Lina Zhao, Peng, Sun and Hao Wang. An Audio Guided Resource Robot Based on Band-pass Filter and Touch Sensors. *Telkomnika*. 2016; 14(3A): 169-177.
[14] Ericka Janet Rechy Ramirez and Huosheng Hu. Bio-signal based control in assistive robots: a survey. *Digital Communication and Networks*. 2015; 1: 85-101.
[15] Koksal Gundogdu, Sumeyye Bayrakdar, and Ibrahim Yucedag. Developing and modelling of voice control system for prosthetic robot arm in medical systems. *Journal of King Saud University - Computer and Information Sciences*. 2017; 30(2): 198-205.
[16] Nianfeng Wang, Kunyi Lao, and Xianmin Zhang. Design and Myoelectric Control of an Anthropomorphic Prosthetic Hand. *Journal of Bionic Engineering*. 2017; 14: 47-59.
[17] E. Hortal, D. Plannelles, A. COsta, E. Ianez, A.Ubeda, J.M. Azorin and E. Fernandez. SVM-based Brain–Machine Interface for controlling a robot arm through four mental tasks. *Neurocomputing*. 2015; 151: 116-121.
[18] Muhammad Ilhamdi Rusydi, Syamsul Huda, Rachmad Amin Putra, Minoru Sasaki, and Febdian Rusydi. *Robot manipulator control using absolutes encoder and electromyography signal*. Asia-Pacific Conference on Intelligent Robot Systems. Tokyo. 2016: 190-194.
[19] Emrehan Yavsan and Aysegul Ucar. Gesture imitation and recognition using Kinect sensor and extreme learning machines. *Measurement*. 2016; 94: 852-861.
[20] Gerad Canal and Sergio, Angulo, Cecilio Escalera. A real-time Human-Robot Interaction system based on gestures for assistive scenarios. *Computer Vision and Image Understanding*. 2016; 140: 65-77.
[21] Giovanni Saggio. Mechanical model of flex sensors used to sense finger movements. *Sensors and Actuators A: Physical*. 2012; 185: 53-58.